

Ca²⁺ Clearance in Visual Motion-Sensitive Neurons of the Fly Studied In Vivo by Sensory Stimulation and UV Photolysis of Caged Ca²⁺

Rafael Kurtz

Lehrstuhl für Neurobiologie, Fakultät für Biologie, Universität Bielefeld, D-33501 Bielefeld, Germany

Submitted 31 October 2003; accepted in final form 2 March 2004

Kurtz, Rafael. Ca²⁺ clearance in visual motion-sensitive neurons of the fly studied in vivo by sensory stimulation and UV photolysis of caged Ca²⁺. *J Neurophysiol* 92: 458–467, 2004; 10.1152/jn.01058.2003. In motion-sensitive visual neurons of the fly, excitatory visual stimulation elicits Ca²⁺ accumulation in dendrites and presynaptic arborizations. Following the cessation of motion stimuli, decay time courses of the cytosolic Ca²⁺ concentration signals measured with fluorescent dyes were faster in fine arborizations compared with the main branches. When indicators with low Ca²⁺ affinity were used, the decay of the Ca²⁺ signals appeared slightly faster than with high affinity dyes, but the dependence of decay kinetics on branch size was preserved. The most parsimonious explanation for faster Ca²⁺ concentration decline in thin branches compared with thick ones is that the velocity of Ca²⁺ clearance is limited by transport mechanisms located in the outer membrane and is thus dependent on the neurite's surface-to-volume ratio. This interpretation was corroborated by UV flash photolysis of caged Ca²⁺ to systematically elicit spatially homogeneous step-like Ca²⁺ concentration increases of varying amplitude. Clearance of Ca²⁺ liberated by this method depended on branch size in the same way as Ca²⁺ accumulated during visual stimulation. Furthermore, the decay time courses of Ca²⁺ signals were only little affected by the amount of Ca²⁺ released by photolysis. Thus Ca²⁺ efflux via the outer membrane is likely to be the main reason for the spatial differences in Ca²⁺ clearance in visual motion-sensitive neurons of the fly.

INTRODUCTION

Neurons often make use of changes in cytosolic calcium concentration ($\Delta[\text{Ca}^{2+}]$) to convert their state of activation into a biochemically readable variable. The most prominent function of $\Delta[\text{Ca}^{2+}]$ is to regulate transmitter release in the presynaptic region (Fossier et al. 1999; Stanley 1997; Südhof 1995; von Gersdorff and Matthews 1999). However, $[\text{Ca}^{2+}]$ also fluctuates in an activity-dependent way in the dendrites of many neurons. Here, Ca²⁺ is suggested to play a role in the short-term regulation of neuronal excitability (adaptation) and in the postsynaptic regulation of synaptic strength on various time scales (Berridge 1998; Sjöström and Nelson 2002; Zucker 1999).

While $[\text{Ca}^{2+}]$ up-regulation has been studied extensively in many neurons, the mechanisms underlying its decline back to a resting level are often not well understood. Large differences in the mechanisms and the kinetics of Ca²⁺ clearance exist both between different cell types and between different cellular regions within individual neurons (Maeda et al. 1999; Majewska et al. 2000). Such differences in Ca²⁺ clearance were found to be functionally significant, e.g., in hippocampal pyramidal neurons

where the location of spines on the dendrite seems to determine both Ca²⁺ dynamics and synaptic plasticity (Holthoff et al. 2002).

Large-field motion-sensitive neurons in the visual system of the fly, the so-called tangential cells (TCs) (Borst and Haag 2002; Egelhaaf and Borst 1993a,b; Egelhaaf et al. 2002; Hausen 1984; Hausen and Egelhaaf 1989), respond to motion in their preferred direction with depolarizations and with $[\text{Ca}^{2+}]$ increases both in their dendrites and in their presynaptic arborizations (Borst and Egelhaaf 1992; Dürr and Egelhaaf 1999; Egelhaaf and Borst 1995; Kurtz et al. 2001; Single and Borst 1998). On their extended dendritic trees, TCs integrate motion signals arriving from local directionally selective input elements in a retinotopic manner. TCs thus generate responses that are fairly specific for certain patterns of optic flow. Such optic flow patterns provide information about the self-motion of the animal and the three-dimensional layout of the environment. TCs synaptically transmit this visual motion information to neurons descending to the fly's motor control centers or to TCs that project to the contralateral half of the visual system. This connectivity forms networks that have been concluded to further increase optic flow specificity (Haag and Borst 2001; Horstmann et al. 2000).

So far, the regulation of presynaptic $[\text{Ca}^{2+}]$ during synaptic transmission between TCs, the involvement of dendritic Ca²⁺ in motion adaptation, and differences in Ca²⁺ dynamics between different types of TCs have been studied (Dürr et al. 2001; Kurtz et al. 2000, 2001). The physiology of $[\text{Ca}^{2+}]$ increases in TCs has been investigated by voltage-clamp experiments in vivo (Haag and Borst 2000), by pharmacological methods in an in vitro preparation (Oertner et al. 2001), and by computer simulations with compartmental models of individual TCs (Borst and Single 2000). In contrast, Ca²⁺ clearance has not yet been investigated thoroughly in TCs.

Here I study, in single TCs in vivo, the time course of the decline of Ca²⁺ fluorescence signals following Ca²⁺ accumulation during excitatory motion stimulation and after release of Ca²⁺ by UV-flash photolysis of caged compounds. Compared with visual motion stimulation, by flash photolysis, $[\text{Ca}^{2+}]$ can be raised in the cytosol much more homogeneously and in a step-like manner. The flash photolysis technique (Nerbonne 1996) is applied here for the first time during in vivo experiments in the neural system of the fly. It may help in the future to elucidate the role of Ca²⁺ in the intact nervous system, e.g., in the context of synaptic transmission and adaptation.

Address for reprint requests and other correspondence: R. Kurtz, Lehrstuhl für Neurobiologie, Fakultät für Biologie, Universität Bielefeld, Postfach 10 01 31, D-33501 Bielefeld, Germany (E-mail: rafael.kurtz@uni-bielefeld.de).

The costs of publication of this article were defrayed in part by the payment of page charges. The article must therefore be hereby marked "advertisement" in accordance with 18 U.S.C. Section 1734 solely to indicate this fact.

METHODS

Membrane potential recordings, Ca²⁺ imaging, and flash photolysis of caged Ca²⁺ were performed in vivo on TCs in the third visual neuropil of the fly, the lobula plate. Identification of individual TCs was based on their receptive field properties, specific characteristics of their electrical responses (see RESULTS), and their anatomy, visualized with fluorescent Ca²⁺ dyes.

TCs were visually stimulated by an LED board, displaying apparent motion squarewave gratings, moving with a temporal frequency of 4 Hz in the preferred direction of the TC. The pattern had a mean luminance of 509 cd/m², a Michelson contrast of 99.3%, and an angular extent of ~50 × 60°, with the larger extent perpendicular to the axis of motion (Kurtz et al. 2001).

All experiments were carried out at room temperature (18–25°C) on female blowflies of the genus *Calliphora*, 1–3 days of age, taken from the department's laboratory stocks. Animal preparation and electrophysiological recording techniques are as previously described in Dürr and Egelhaaf (1999) and Kurtz et al. (2001).

Ca²⁺ imaging

$\Delta[\text{Ca}^{2+}]$ in single TCs was estimated by imaging fluorescence changes of an intracellular Ca²⁺-sensitive dye. The dye was iontophoretically injected into single neurons from the tip of sharp recording electrodes by applying a hyperpolarizing current of 1–3 nA for 5–10 min and left to diffuse throughout the cytoplasm for ≥ 5 min. Typically, the tip of the electrode contained (in mM) 9 Oregon-Green 488 BAPTA-1 hexapotassium salt (OG-1; Molecular Probes), 51 NP-EGTA tetrapotassium salt (Molecular Probes), and 5 KOH (Merck). The shaft of the electrode was filled with 1 M KCl (Merck). In some experiments, different concentrations of OG-1 (range, 5–19 mM) and NP-EGTA (range, 23–58 mM) were used, or DMNP-EDTA (35 mM; Molecular Probes) was included instead of NP-EGTA in the electrode tip. In the experiments that led to the data shown in Fig. 3, the electrode tips contained (in mM) 33.3 KCl, 1.7 KOH, and 33.3 HEPES (Sigma), pH 7.3, and one of the following fura-based Ca²⁺ dyes (20 mM), which differed from each other in Ca²⁺ binding affinity: fura-2 pentapotassium salt, Bis-fura 2 hexapotassium salt, or fura-6F pentapotassium salt (all from Molecular Probes).

Epifluorescence measurements were performed with an upright microscope (Axioskop FS, Zeiss) with a water immersion objective (Achromplan 40×, NA 0.75, Zeiss). The excitation light source was a Hg arc lamp (HBO 100 W, Osram). Excitation light was band-pass filtered at 380 ± 5 nm for the fura-based Ca²⁺ dyes and at 475 ± 20 nm for OG-1. Emitted light passed through a 410-nm dichroic mirror and a 515 ± 15 band-pass filter for fura-imaging. A 500-nm dichroic and a 530 ± 25 band-pass filter was used for OG-1. A cooled frame-transfer CCD-camera (Quantix 57, Photometrics) controlled by PMIS software (GKR Computer Consulting) was used to acquire 128 × 128 pixel images (512 × 512 chip size, binning factor 4) at a frame rate of 14 Hz. The measurements shown in Fig. 3 were performed either with 32 × 32 pixel images (512 × 512 chip, binning factor 16), acquired at a frame rate of 21 Hz, or with another type of CCD-camera (PXL, Photometrics) and 10 × 10 pixel images (160 × 160 subregion of the 512 × 512 chip, binning factor 16), acquired at a frame rate of 40 Hz. The low spatial resolution of these recordings was acceptable because differentiation between cellular subregions was not necessary for the conclusions drawn from the results shown in Fig. 3.

UV flash photolysis of caged Ca²⁺

I adapted the flash photolysis technique to the requirements of the in vivo preparation of the fly. Single TCs were filled with a caged Ca²⁺ compound by iontophoresis from the electrode tip (see above for electrode solutions). To release Ca²⁺ into the cytosol, a brief flash (pulse length, ~1 ms) of light, generated by a Xenon flash lamp

(JML-C2, Rapp Optoelectronics), was filtered ($\lambda < 380$ nm) and delivered to the neuron via a quartz light guide with a diameter of 100 or 200 μm . Ca²⁺ was photoreleased during Ca²⁺ fluorescence data acquisition. A single image capturing the light flash had to be blanked from the sequence. In about one-half of the experiments, the membrane potential of the TC was recorded during flash photolysis of caged Ca²⁺. A brief visual response to the UV flash was observed. This is due to flash light shining through the head capsule and exciting the photoreceptors. In some experiments, we filtered the flash light with a cut-off at even shorter wavelengths ($\lambda < 360$ nm) to attenuate these unwanted visual responses. This, however, also decreased the amount of photoreleased Ca²⁺. For the questions addressed in this paper, a brief visual excitation by the UV flash is not critical, because $\Delta[\text{Ca}^{2+}]$ induced by this visual excitation is much weaker than $\Delta[\text{Ca}^{2+}]$ induced by release from the caged compound. I nevertheless made efforts to minimize visual excitation by the UV flash because it is planned to use flash photolysis in future studies on the role of Ca²⁺ in synaptic transmission and adaptation.

In most of my experiments, I used NP-EGTA (Ellis-Davies and Kaplan 1994). This caged compound has a high selectivity for Ca²⁺. In contrast, DMNP-EDTA, which I used in some of my experiments, has a considerable affinity for Mg²⁺ (Kaplan and Ellis-Davies 1988). Mg²⁺ is typically present in the cytosol at higher concentrations than Ca²⁺ under physiological conditions. Since the applied Ca²⁺ indicators respond weakly to Mg²⁺ concentration changes (Haugland 2002), release of Mg²⁺ and a minor contribution of Mg²⁺ to the measured fluorescence signal during flash photolysis cannot be excluded. However, in my experiments with flash photolysis, I did not observe any obvious differences between NP-EGTA and DMNP-EDTA. Although DMNP-EDTA produced similar results to NP-EGTA, I routinely used the latter because of its higher aqueous solubility, which facilitates filling of electrode tips with high concentrations of the compound.

Data analysis

Routines written in C (Borland), Matlab (The Mathworks), or PMIS (GKR Computer Consulting) were used for data analysis. The change in fluorescence divided by the fluorescence intensity at the beginning of an image series ($\Delta F/F$) served as a relative measure of $\Delta[\text{Ca}^{2+}]$ (Vranesic and Knöpfel 1991). The range in which $\Delta F/F$ is proportional to $\Delta[\text{Ca}^{2+}]$ depends on concentration, affinity, and dynamic range of the Ca²⁺ dye and on the resting $[\text{Ca}^{2+}]$. The latter has been estimated by ratiometric Ca²⁺ imaging to be 20–60 nM in vivo (Egelhaaf and Borst 1995), to be 50–180 nM in an in vitro preparation of the fly brain (Oertner et al. 2001), and to rise two- to threefold during several seconds of sensory or electrical stimulation. Increases in this range are likely to lie well within the linear range of the Ca²⁺ dyes used in our study (Lev-Ram et al. 1992; Thomas et al. 2000). To facilitate comparisons of $\Delta F/F$ between regions with different fluorescence intensity, background fluorescence in a region outside the stained neuronal structures was determined for each image and subtracted from the raw fluorescence images. When Ca²⁺ fluorescence in the dendrite was evaluated (data shown in Fig. 8), I refrained from background correction in two neurons, because the camera images did not contain large enough areas completely devoid of cellular structures. Comparisons of $\Delta F/F$ between different regions were always performed by selecting mask areas within one image series, instead of making comparisons between different series. This was done to ensure that the neurites that were compared were in the same focal plane, i.e., in similar depth below tissue surface, and were thus illuminated by the photolysis flash with similar efficiency.

For illustrative reasons, the false color-coded images shown in the figures were not background-corrected and were smoothed by a median filter. The median filter operation replaces each pixel with the median value of the center pixel and its eight neighbor pixels.

When fura-based dyes were used (data shown in Figs. 3 and 4), increases in $[\text{Ca}^{2+}]$ led to a decrease in $\Delta F/F$. I multiplied these $\Delta F/F$

values by -1 to facilitate comparisons with data acquired with the use of OG-1.

To compare $[Ca^{2+}]$ kinetics, the $\Delta F/F$ traces were normalized by setting the average $\Delta F/F$ in a time window of 1 s preceding stimulation to zero and setting the starting point of the $\Delta F/F$ decay following stimulation to one.

A function consisting of a single exponential and a linear time-dependent term was fitted to normalized $\Delta F/F$ decay time courses: $\Delta F/F(t) = e^{(-t/\tau)} + c \times t$.

The fit usually started with the first or the second data point after cessation of motion stimulation (to account for cell-to-cell differences in response latency), or, in experiments with caged Ca^{2+} , with the first data point after the UV flash. In about one-quarter of the experiments with flash photolysis, however, there was an initial rapid decline of $\Delta F/F$ directly following the UV flash, continued by a slower decline. The reason for this might be rapid rebinding of released Ca^{2+} to free chelator molecules (Escobar et al. 1997). In such cases, the second or the third instead of the first data point after flash photolysis was normalized to one, and the fit was started from this value. The additive time-dependent linear term in Eq. 1 accounts for drift in the data, e.g., originating from dye bleaching. Thus this term often reduced the mean squared errors of the fits by more than one-third. For one neuron, however, this term was set to zero since it otherwise resulted in fits with extremely long τ values. Throughout the whole study, I obtained qualitatively the same results when all fits were performed with single-exponential decay functions without an additive linear component (data not shown). In several cases, double-exponential fits probably would have yielded better fits (i.e., lower mean squared errors). I nevertheless used single-exponential fits throughout this study to allow for a better quantitative comparability of the data.

RESULTS

Experiments were performed on neurons of the horizontal system (HS) and the vertical system (VS), two prominent and well-studied TC classes comprising 3 and 10 neurons, respectively. Stimulation with visual motion elicits graded shifts of the membrane potential that remain prominent in the axon close to the neurons' synaptic output regions far from the dendrite (Hausen 1982a,b; Hengstenberg 1982; Hengstenberg et al. 1982). As is shown in Fig. 1A for a VS cell, spike-like fast membrane depolarizations, which appear—unlike “ordinary” action potentials—very variable in amplitude, are superimposed on the graded depolarizations. The membrane potential responses are accompanied by $\Delta[Ca^{2+}]$, both in the dendrite and in the presynaptic region (Borst and Egelhaaf 1992; Egelhaaf and Borst 1995). During motion in the neurons' preferred direction (PD), downward motion in the case of VS, the membrane potential depolarizes and $[Ca^{2+}]$ rises, as indicated by an increase in $\Delta F/F$ during excitation of the Ca^{2+} -sensitive fluorescent dye OG-1 (see Fig. 1, A and B). Motion in the opposite direction, the so-called null direction (ND), leads to membrane hyperpolarization (Fig. 1A) and to a decrease in $\Delta F/F$. This decrease in $\Delta F/F$ is much weaker than the increase during PD motion in the presynaptic region of the cell and often not detectable at all in the dendrites of VS and HS cells (data not shown, see Borst and Single 2000; Dürr et al. 2001; Kurtz et al. 2001; Single and Borst 1998).

Differences in Ca^{2+} signal decay kinetics correlated with the size of neurites

Following the cessation of excitatory motion stimuli, the velocity with which accumulated Ca^{2+} is cleared from the

cytosol differs between the subregions of the terminal. At fine presynaptic endings, the decrease of $\Delta F/F$ to the resting level is faster than in the larger-diameter proximal axonal segment (Fig. 1B). Best fits of a single-exponential decay to the normalized individual traces yielded decay time constants (τ values) of 0.7 s for the mask area covering the endings and 1.4 s for the proximal axonal mask (and intermediate in a whole-area mask, see Fig. 1B). The respective values for the mean time course of normalized individual traces ($n = 10$) were 1.0 and 1.5 s (Fig. 1B).

A similar analysis was performed for the presynaptic regions of seven VS cells and three HS cells: τ values were determined for the $\Delta F/F$ decay in two mask areas similar to those in Fig. 1B, covering either fine presynaptic endings or a proximal axonal segment. These τ values were divided by the τ value for a mask covering the whole presynaptic region. This normalization facilitates the comparison of data from different neurons with differences in absolute $\Delta F/F$ decay times, which may result from different presynaptic branching patterns and variability in the exact layout of the mask areas. In Fig. 2, the logarithms of the relative τ values of the $\Delta F/F$ decay times are plotted. Thus equal deviations from zero represent equal relations to the reference value, regardless of the direction of the deviation. $\Delta F/F$ decay τ values at the fine presynaptic endings were on average 10.5% shorter than the reference set by the whole area mask. In contrast, the τ values at the proximal axonal segment were on average 41.2% longer than the reference value.

Thus Ca^{2+} clearance appears to become faster with decreasing diameter of a presynaptic arborization, i.e., the closer one approaches the actual sites of transmitter release.

Impact of exogenous Ca^{2+} buffer on Ca^{2+} kinetics

Any Ca^{2+} buffer added to a neuron's endogenous buffers alters the temporal profile of $[Ca^{2+}]$ changes. Any Ca^{2+} -sensitive fluorescence dye, such as OG-1, is a Ca^{2+} buffer that competes with internal Ca^{2+} buffers and might, depending on its affinity and diffusibility relative to that of internal buffers, not only lead to a longer retention of Ca^{2+} in the cytosol, but also affect Ca^{2+} diffusion (Sabatini et al. 2002; Sala and Hernandez-Cruz 1990). Thus for neurons with largely unknown internal buffer properties—as is the case for TCs—it is hard to predict whether the addition of a Ca^{2+} -sensitive dye amplifies or attenuates any differences in $[Ca^{2+}]$ time courses in arborizations of different size. To test for effects of added buffers on $[Ca^{2+}]$ time courses, I compared Ca^{2+} signals measured with Ca^{2+} -sensitive dyes that differ in their affinity for Ca^{2+} . We used the dyes fura-2, bis-fura 2, and fura-6F, which differ in their Ca^{2+} binding properties, as characterized by dissociation constants of 145 nM, 370 nM, and 5.3 μ M, respectively (k_d values reported in Haugland 2002; determined in buffered salines, actual values inside cells may differ, see e.g., Thomas et al. 2000). Apart from the different Ca^{2+} binding affinities, the dyes are very similar in their fluorescence properties.

The time courses of $\Delta F/F$ decrease after motion offset are generally faster when measured with low-affinity dyes compared with the time courses obtained with high-affinity dyes (Fig. 3). The $\Delta F/F$ decay is slightly faster when measured with the medium-affinity dye bisfura-2 than when measured with the high-

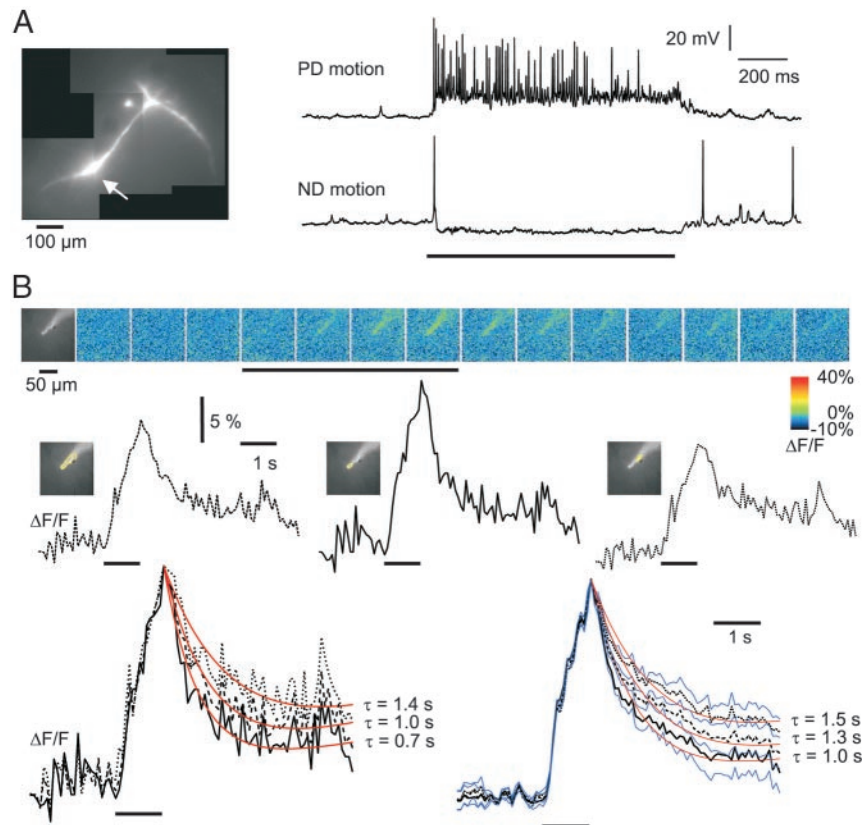


FIG. 1. Responses of a vertical system (VS) neuron to visual motion. *A: left:* VS neuron filled with Oregon-Green 488 BAPTA-1 hexapotassium salt (OG-1) assembled from several images taken by a CCD camera on a fluorescence microscope in the living animal. The neuron is either VS2 or VS3, which are very similar in their structure and in their functional properties (termed collectively VS2/3 in the following) (Krapp et al. 1998). The bifurcated dendrite of the neuron is visible to the right (dorsal branch is partly occluded by a tracheae). The axon with the soma attached to it via a thin neurite ends in the neuron's synaptic output region in the bottom left of image. Former position of the recording electrode is still visible as a bright spot in the bottom part of the axon (see arrow). *Right:* electrical response of the VS neuron to motion of a grating in the preferred downward direction (PD) and in the opposite direction (ND). Pattern motion is indicated by the horizontal bar. *B: Ca²⁺ accumulation in the presynaptic output region of VS2/3 during PD motion and Ca²⁺ clearance after the cessation of motion. Top:* raw fluorescence image and series of images showing $\Delta F/F$ of OG-1 under fluorescence excitation in a false-color code. Every 4th image out of an excerpt from the original series (acquisition rate 14 Hz) is shown, with pattern motion indicated by the horizontal bar. *Middle:* individual time courses of $\Delta F/F$ quantified in 3 different mask areas, as indicated by the yellow line in the fluorescence images (*insets*). *Bottom left:* same individual traces (with corresponding line styles) now normalized to the 1st datapoint after cessation of visual motion. Exponential decay functions are fitted to curves (red lines). Decay is fastest in a mask area covering only the very tip of the axonal ending in the presynaptic region (solid line), slowest in a mask area on proximal axonal shaft (dotted line), and intermediate when determined in a mask area covering the entire presynaptic region of the neuron (dashed line). *Bottom right:* same analysis applied to mean time courses averaged from 10 normalized traces recorded in the single VS2/3 cell. Line styles as before, with additional blue lines, depicting SE. For better clarity, the *top* and *bottom* traces are shown with the SE only to its *top* and *bottom*, respectively.

affinity dye fura-2 (cell averages: $\tau = 2.1$ vs. 2.8 s, $n = 5/8$) and considerably faster when measured with the low-affinity dye fura-6F ($\tau = 0.9$ s, $n = 3$). In addition, the increase of $\Delta F/F$ during motion stimulation appears to be slightly faster with fura-6F compared with the other two dyes (Fig. 3).

It should be noted that, irrespective of the impact of exogenous Ca²⁺ buffer on $\Delta F/F$ time courses, $\Delta F/F$ decay times differed in arborizations of different size for dyes of any affinity. As shown before for OG-1 ($k_d = 170$ nM; Fig. 1B), Ca²⁺ clearance measured with the low-affinity dye fura-6F ($k_d = 5.3$ μ M) is faster when determined in an area covering fine branches in the presynaptic region compared with an area covering the proximal axonal segment ($\tau = 0.7$ vs. 1.0 s, see Fig. 4). $\Delta F/F$ time courses were measured with fura-6F in two other VS cells. In both cells, the decay of $\Delta F/F$ following visual stimulation was faster in thin presynaptic arborizations than in thick ones, with $\tau = 1.0$ vs. 1.9 s

in one cell and 0.4 vs. 1.2 s in the other cell. Thus the branch size-dependent difference in $\Delta F/F$ decay times is not merely an artifact of increasing buffer capacity by adding Ca²⁺ buffer to the cytosol, but can be expected to exist also under undisturbed cytosolic conditions.

Spatial differences in Ca²⁺ signal amplitudes during visual stimulation

The most parsimonious explanation for the dependence of Ca²⁺ fluorescence decay time on the diameter of neuritic arborizations is that the rate-limiting step in Ca²⁺ clearance is extrusion through the plasma membrane by physiological mechanisms such as the Na⁺/Ca²⁺ exchanger (Blaustein and Lederer 1999) or Ca²⁺ ATPase (Carafoli and Brini 2000). The high surface area-to-volume ratio of small-diameter arboriza-

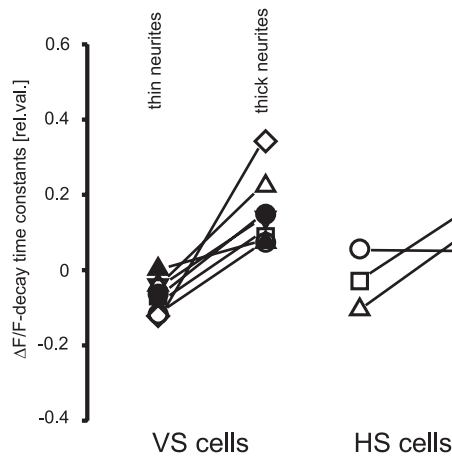


FIG. 2. Comparison of decay times of Ca^{2+} signals in neurites of different size in the presynaptic region of VS and horizontal system (HS) neurons. For each cell, $\Delta F/F$ decay τ values were determined by fits to averaged normalized $\Delta F/F$ time courses following cessation of 1-s stimulus motion (see Fig. 1). $\Delta F/F$ decay was determined in 3 mask areas: the 1st laid on a region where thin endings are located, the 2nd on an adjacent region with thicker branches, and the 3rd covered the entire presynaptic area. To highlight the relative difference between thin and thick arborizations, decay times obtained for the 1st and 2nd mask were divided by that for the 3rd mask and plotted logarithmically. Thus 0 indicates time constants identical to those obtained for the whole area mask of the particular cell, whereas positive and negative values denote longer and shorter time constants, respectively.

tions would then favor a faster $[\text{Ca}^{2+}]$ decay than in large branches (Holthoff et al. 2002; Lev-Ram et al. 1992).

The branch size–dependent differences in $\Delta F/F$ decay times in presynaptic regions of TCs are in accordance with the dependence of Ca^{2+} clearance on the surface-to-volume ratio. However, when investigating the removal of Ca^{2+} from the cytosol after its accumulation during sensory stimulation, one major caveat is that Ca^{2+} may rise to different concentrations in different arborizations (Dürr and Egelhaaf 1999; Holthoff et al. 2002). This has to be expected since Ca^{2+} influx also proceeds via the outer membrane and diffusion may not be fast enough to equilibrate any arising $[\text{Ca}^{2+}]$ gradient rapidly enough. Therefore instead of surface-to-volume ratio as the determinant of the rate of Ca^{2+} clearance, other mechanisms involved in the removal of Ca^{2+} from the cytosol could produce an apparent dependency on branch diameter, while actually being dependent on $[\text{Ca}^{2+}]$ itself. Such a concentration dependence of Ca^{2+} clearance could produce faster Ca^{2+} clearance in arborizations with higher $[\text{Ca}^{2+}]$, i.e., in small-diameter branches. For example, concentration-dependence of Ca^{2+} clearance could be due to saturation of intrinsic Ca^{2+} buffers, nonlinear binding of Ca^{2+} to Ca^{2+} buffers and Ca^{2+} pumps, or uptake into mitochondria or the endoplasmic reticulum at high $[\text{Ca}^{2+}]$ (Herrington et al. 1996; Maeda et al. 1999; Medler and Gleason 2002).

Figure 5A shows that nonuniform $\Delta F/F$ increases complicate the interpretation of $[\text{Ca}^{2+}]$ decay kinetics in TCs following visual stimulation, in particular, if there are many side branches in the presynaptic region, as is often the case in VS1. In fine presynaptic branches, $\Delta F/F$ rose to higher values than in thick ones: The peak $\Delta F/F$ value after 1 s of stimulus motion was 15% in fine presynaptic endings of the VS1 cell but only 8% in the adjacent axonal shaft.

Ca^{2+} clearance following flash photolysis of caged Ca^{2+}

To compare Ca^{2+} clearance starting from similar concentration levels in different cellular regions, I artificially increased $[\text{Ca}^{2+}]$ in a step-like manner by UV-flash photolysis of a caged Ca^{2+} compound (NP-EGTA or DMNP) injected iontophoretically into single TCs during electrical recordings. In contrast to visual stimulation, $[\text{Ca}^{2+}]$ can be increased by this method in a spatially homogeneous way, provided that Ca^{2+} cage equilibrates throughout the cell, and UV illumination is spatially homogeneous. The first criterion was met by waiting ≥ 5 min before starting the experiment after the iontophoretic application of the Ca^{2+} cage and the fluorescent Ca^{2+} dye. The second requirement was met since I only made comparisons between mask areas within a very restricted region.

As shown by Ca^{2+} imaging, UV photolysis elicits step-like increases in $\Delta F/F$, which, as expected, differ in size much less than $\Delta F/F$ increases obtained by sensory stimulation (Fig. 5B). The actual $[\text{Ca}^{2+}]$ steps might be even more similar in size than the measured ones, since in single-wavelength Ca^{2+} measurements, signals in weakly stained thin arborizations tend to be underestimated even with background correction (Dürr and Egelhaaf 1999; Haag and Borst 2000; Lev-Ram et al. 1992).

Ca^{2+} released by flash photolysis declines back to baseline concentration levels with a time course similar to Ca^{2+} accumulated by visual stimulation. Analogous to what was found for Ca^{2+} signals during visual stimulation, the recovery of $\Delta F/F$ after flash photolysis of caged Ca^{2+} differs between arborizations of different size: This is depicted in Fig. 6 for the same VS neuron as was shown in Fig. 1, using similar mask areas to those used for the analysis of Ca^{2+} signals in response to visual stimulation. For averaged normalized traces, the corresponding τ values of the $\Delta F/F$ decay after flash photolysis are 0.5 s for masks covering fine branches, 1.1 s for masks covering thicker ones, and 0.9 s for masks covering the entire presynaptic region (Fig. 6). As was done for the Ca^{2+} signals elicited by visual stimulation, decay τ values were determined for Ca^{2+} signals elicited by flash photolysis in seven VS and two HS neurons. These values were determined for fine and for thick branches and were normalized with respect to the corresponding whole area mask. Similar to visual stimulation, Ca^{2+}

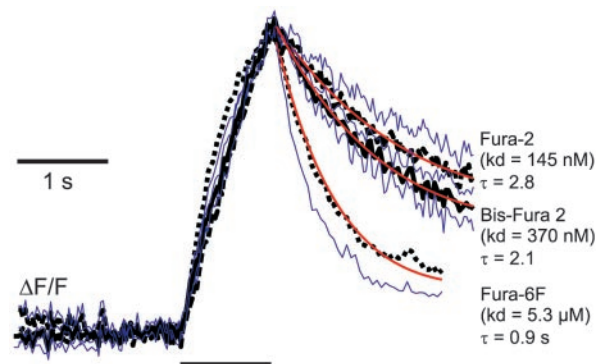


FIG. 3. Impact of Ca^{2+} dye affinity on time courses of presynaptic $\Delta F/F$. Fluorescent dyes with different dissociation constants (see k_d values) were used to report $\Delta[\text{Ca}^{2+}]$ during motion stimulation (horizontal bar). Mean traces of normalized $\Delta F/F$ time courses were 1st determined for each neuron and subsequently averaged for 8, 5, and 3 VS neurons filled with fura-2, Bis-fura 2, and fura-6F, respectively (blue lines; SE). Velocity of measured $\Delta F/F$ decay after cessation of stimulus motion slows down with increasing dye affinity (see exponential fits indicated by red lines and τ values).

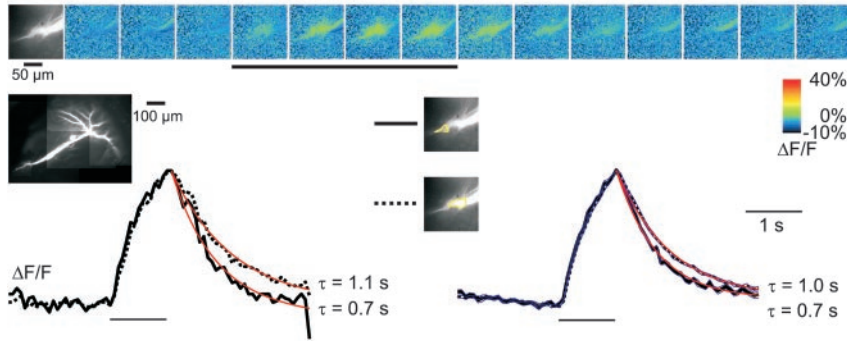


FIG. 4. Spatial differences in presynaptic Ca²⁺ dynamics measured with the low-affinity dye fura-6F. *Top*: raw fluorescence image and series of images showing $\Delta F/F$ in a false-color code, taken at the presynaptic region of a VS1 cell (see compound image) during presentation of PD motion (horizontal bar). *Bottom left*: normalized time courses of individual $\Delta F/F$ quantified in 2 different mask areas (see insets for line styles) with exponential functions fitted to the $\Delta F/F$ decay (red lines). *Bottom right*: averaged normalized $\Delta F/F$ time courses with fits (red lines) and SE (blue lines, $n = 17$). Details of data presentation as in Fig. 1.

clearance after UV flash photolysis of caged Ca²⁺ was found to be considerably faster in fine presynaptic arborizations compared with thick ones (Fig. 7). In relation to the reference set by the whole area mask, $\Delta F/F$ decay τ values were on average 23.4% shorter when determined at fine presynaptic endings but on average 13.7% longer when determined at thick branches.

Ca²⁺ clearance in the dendrites of TCs

In analogy to my analysis of Ca²⁺ clearance in presynaptic arborizations, I also tested whether the kinetics of $\Delta F/F$ decay

after visual stimulation and after flash photolysis of caged Ca²⁺ differs between dendrites of different size in the main input region of TCs.

Dendritic Ca²⁺ accumulation during excitatory visual stimulation is correlated in its magnitude and in its kinetics with an afterhyperpolarization (AHP), leading to direction-selective motion adaptation (Harris et al. 2000; Kurtz et al. 2000). Since Ca²⁺ was found to be associated with adaptation in HS and centrifugal horizontal (CH) neurons, I additionally included the latter type of TCs into my analysis. There are two CH neurons, a dorsal (DCH) and a ventral one (VCH), which are both sensitive to horizontal motion and form dendrodendritic inhibitory synapses in the lobula plate (Egelhaaf et al. 1993; Gauck et al. 1997; Warzecha et al. 1993). Thus “dendritic” Ca²⁺ signals in CH neurons may also play a role in regulating transmitter release.

Both after cessation of visual motion and after Ca²⁺ release by flash photolysis, faster $\Delta F/F$ decay time courses were found in mask areas covering thin distal dendrites than when thicker proximal ones were selected (Fig. 8). Whereas such a difference was found for all neurons tested with flash photolysis, the results obtained with visual stimulation were less consistent. In five cells, $\Delta F/F$ decay was faster in thin than in thick branches, in one cell it was slower, and in three cells there was virtually no difference (Fig. 8, see legend for cell types). Interestingly, the cells with slower decay in thin neurites or no difference between neurites were all CH neurons. This difference between cell types might be due to methodological reasons (see DISCUSSION), or it might reflect a principle difference in dendritic Ca²⁺ regulation between different cell types. It is important to note in this context that CH neurons deviate from VS and HS neurons in their dendritic properties. Whereas the latter receive input at chemical synapses from local visual-motion-sensitive elements, CH cells are provided with visual motion input from HS cells via electrical synapses (Haag and Borst 2002). Moreover, whereas the dendrite of VS and HS cells is a purely postsynaptic structure, CH cells possess dendrodendritic inhibitory synapses by which they transmit motion information to other TCs (Egelhaaf et al. 1993; Gauck et al. 1997; Warzecha et al. 1993). Thus “dendritic” Ca²⁺ signals in CH neurons may also play a role in regulating transmitter release.

Independence of Ca²⁺ clearance from [Ca²⁺]

The time course of Ca²⁺ clearance appeared faster in thin than in thick branches both in the dendrite and in the output area of TCs. For VS and HS neurons, this held true, regardless of whether the Ca²⁺ accumulation was caused by sensory input

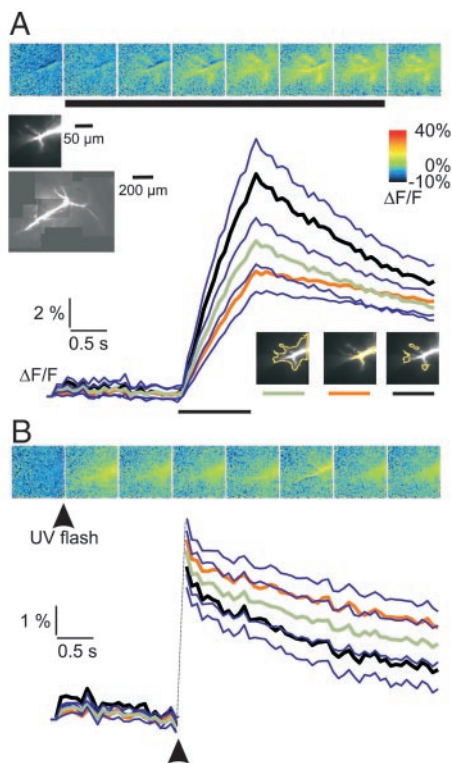


FIG. 5. Changes in presynaptic [Ca²⁺] during visual stimulation and during flash photolysis of caged Ca²⁺. *A*: false-color images and time courses of Ca²⁺ fluorescence in the presynaptic region of VS1 during presentation of PD motion (horizontal bar). Ca²⁺ signal is compared for 3 different mask areas (see insets). Averaged $\Delta F/F$ traces ($n = 8$) indicate that [Ca²⁺] rises to higher values in the thin tips of the presynaptic arborization (black line) than in the thicker main branch (red line). *B*: As in *A*, but during UV flash photolysis of NP-EGTA, filled iontophoretically into the neuron. The image taken during the UV flash is overexposed and had to be blanked; corresponding part of averaged $\Delta F/F$ traces ($n = 15$) is bridged by a thin dotted line. $\Delta F/F$ peak immediately after UV flash has a similar amplitude in the different mask areas (line colors as in *A*). Details of data presentation similar to Fig. 1, but with false-color series showing every 2nd image out of an excerpt from the original series.

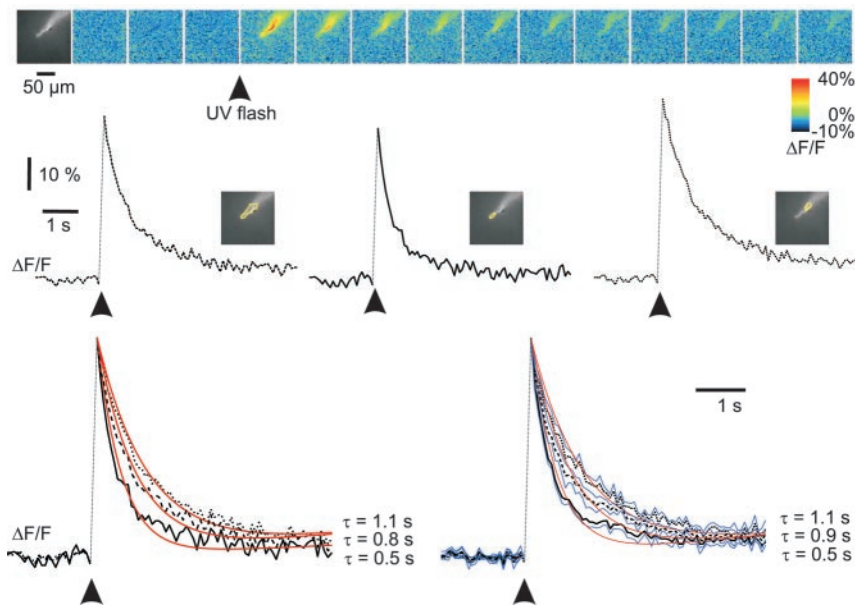


FIG. 6. Spatial differences in the dynamics of the pre-synaptic $\Delta F/F$ decay following flash photolysis of caged Ca^{2+} . Series of false-color coded images of Ca^{2+} fluorescence (top), individual traces of the $\Delta F/F$ time course for 3 different mask areas (middle), normalized $\Delta F/F$ traces (bottom left), and average of normalized $\Delta F/F$ traces (bottom right; $n = 6$) for the same cell as in Fig. 1. Data presentation as in Fig. 1.

to the neuron or by release from a photolabile Ca^{2+} buffer. Since in the latter case $[\text{Ca}^{2+}]$ decay can be expected to start from nearly the same concentration irrespective of neurite size, the differences in $\Delta F/F$ decay times are most likely explained by a dependence of Ca^{2+} clearance on surface area-to-volume ratio. However, this explanation does not exclude an additional contribution of concentration-dependent Ca^{2+} clearance mechanisms.

Ca^{2+} release from caged compounds offers the opportunity to vary the amount of Ca^{2+} liberated inside the cell by controlling the intensity of the UV flash. To test whether the time constant of Ca^{2+} clearance decreases with the amount of Ca^{2+} that is to be removed from the cytosol, I

elicited steps to different $[\text{Ca}^{2+}]$ by photolysis with various flash intensities (Fig. 9A). This type of concentration dependence of the time constant would be expected if additional clearance mechanisms were recruited by high $[\text{Ca}^{2+}]$. However, I found that there is a tendency toward slower $\Delta F/F$ decay time courses in response to larger $[\text{Ca}^{2+}]$ steps for the cell shown already in Figs. 1 and 6 (Fig. 9A). In Fig. 9B, the results of similar analyses performed with 10 cells are plotted. For each cell, individual $\Delta F/F$ and τ values were normalized to their mean values to center the data points for each cell in the plot. On the whole, $\Delta F/F$ decay times are either independent of initial $\Delta F/F$ or may increase slightly with increasing initial values. This finding is in contrast to what would be expected if concentration dependence of Ca^{2+} clearance rather than surface-to-volume ratio was the reason for spatial differences in $\Delta F/F$ decay times.

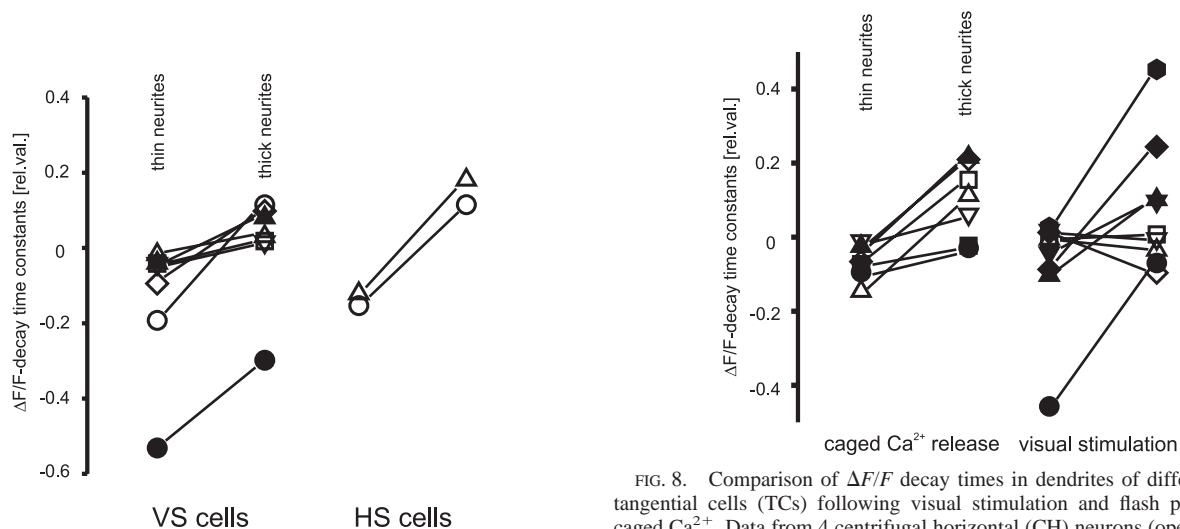


FIG. 7. Comparison of $\Delta F/F$ decay times in neurites of different size in the presynaptic region of VS and HS neurons following flash photolysis of caged Ca^{2+} . For details on data evaluation and presentation, see Fig. 2.

FIG. 8. Comparison of $\Delta F/F$ decay times in dendrites of different size in tangential cells (TCs) following visual stimulation and flash photolysis of caged Ca^{2+} . Data from 4 centrifugal horizontal (CH) neurons (open symbols), 2 HS neurons (solid triangles), and 4 VS neurons (solid circles, squares, and hexagons) are presented. Same symbols represent same cells studied both during visual stimulation and with flash photolysis. For details on data evaluation and presentation, see Fig. 2.

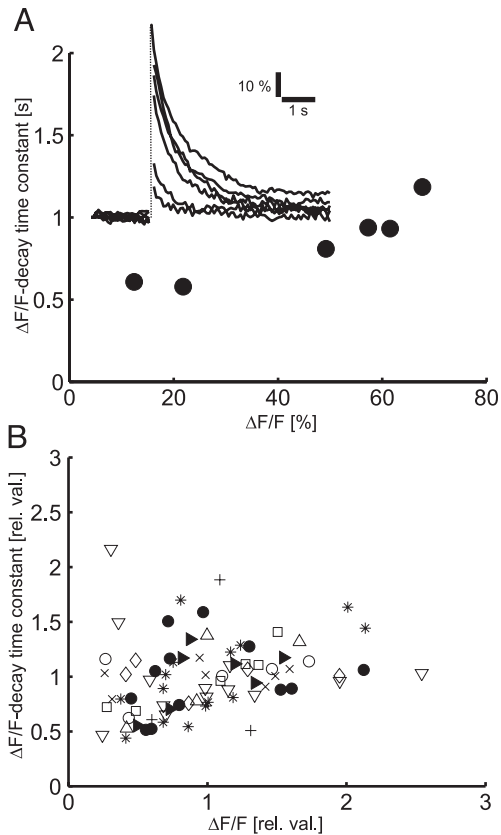


FIG. 9. $\Delta F/F$ decay times following photo release of various amounts of caged Ca^{2+} in the presynaptic region of TCs. *A*: in a single VS neuron (same cell as in Fig. 1), $[\text{Ca}^{2+}]$ peaks with different amplitudes (*inset*) were elicited by varying the intensity of the UV flash. $\Delta F/F$ was measured in a mask area covering the entire presynaptic region. For each trace, the decay time constant is plotted against the corresponding peak in $\Delta F/F$. *B*: same analysis as in *A* was performed with 2 HS neurons (filled symbols) and 8 VS neurons (all other symbols; open squares: data from *A*). Data sets have been centered in the plot by normalizing $\Delta F/F$ decay time constants and Ca^{2+} fluorescence values to respective mean values of each of the cells. The same symbols denote data obtained from the same cell.

DISCUSSION

TCs in the lobula plate of flies respond to visual motion not only with fluctuations in their membrane potential but also with $\Delta[\text{Ca}^{2+}]$ in dendritic and presynaptic arborizations. Ca^{2+} removal from the cytosol, following its accumulation after visual motion stimulation, operates faster in fine arborizations than in large-diameter neurites. This finding is compatible with regulation of Ca^{2+} clearance by mechanisms located in the outer membrane. However, just from the inspection of sensory-evoked $\Delta[\text{Ca}^{2+}]$, alternative explanations of different decay time courses can hardly be refuted, because the concentration level of Ca^{2+} reached during visual stimulation differs between cellular subregions. Thus clearance mechanisms working more effectively once a certain level of $[\text{Ca}^{2+}]$ is reached or saturation of endogenous Ca^{2+} buffers would also lead to different $[\text{Ca}^{2+}]$ decay times. Therefore I applied UV flash photolysis to raise $[\text{Ca}^{2+}]$ to certain levels, which are—in contrast to those during sensory stimulation—similar in different arborizations. Ca^{2+} clearance remained faster in thin branches than in thick ones. Furthermore, decay times are largely independent of the level of $[\text{Ca}^{2+}]$. The latter findings speak against a concentration dependence of Ca^{2+} clearance and confirm a major role of

Ca^{2+} extrusion via mechanisms located in the outer membrane. However, if a mechanism such as the density of intracellular Ca^{2+} stores scales with membrane surface, it cannot be ruled out as a reason for spatial differences in clearance rate. To do so and to distinguish between different mechanisms of Ca^{2+} extrusion via the outer membrane, such as a $\text{Na}^+/\text{Ca}^{2+}$ exchanger or the Ca^{2+} -ATPase, pharmacological methods would have to be applied. These, however, are difficult to use in an *in vivo* preparation, since solution changes reach neurons in intact tissue only slowly. Moreover, chemicals would not influence exclusively TCs, but also more peripheral cells, thus rendering it hard to draw strong conclusions. However, in a study where ryanodine, caffeine, and thapsigargin were applied to an *in vitro* preparation of the fly optic lobes, no indications of calcium regulation by internal stores were found in TCs (Oertner et al. 2001). Stores insensitive to these drugs may, of course, play a role. In the same study, a slow return to resting calcium in low sodium saline hints to an involvement of $\text{Na}^+/\text{Ca}^{2+}$ exchangers in calcium clearance.

Methodological considerations

A proper evaluation of spatial differences in $[\text{Ca}^{2+}]$ dynamics depends critically on the temporal and spatial resolution of Ca^{2+} imaging. The resolution achieved in this study (spatial: $\sim 1.2 \mu\text{m}$; temporal: 14 Hz) was sufficiently high to show that the decay time courses of $\Delta F/F$ after the cessation of brief motion stimuli differ between arborizations of different size. Spatial resolution might, however, be compromised considerably by light scattering. This problem is largest when fluorescent structures are close-packed. This might be one reason why differences in Ca^{2+} dynamics during visual stimulation were detected in VS and HS neurons but were not detected in CH cells, the dendrite of which is more extensively branched.

Differences in surface-to-volume ratio serve as a parsimonious explanation for shorter Ca^{2+} decay times in thin than in thick neurites. However, how can this explanation be brought in line with the fact that the temporal profiles of $\Delta F/F$ rises appear independent of branch size, although Ca^{2+} enters the cell exclusively, or at least to a large extent, via the outer membrane (Haag and Borst 2000; Oertner et al. 2001; Single and Borst 2002)? The reason seems to be that $\Delta F/F$ levels reached during short motion stimuli are far from steady state, and the rise in $\Delta F/F$ is still in its initial quasi-linear phase. Accordingly, time constants for $\Delta F/F$ rises during short-term visual stimulation cannot properly be assessed. Hence, responses to longer motion stimuli, driving $[\text{Ca}^{2+}]$ to its steady state, may display branch-size dependent differences in their rise time. Such differences were indeed found in the dendrites of HS and CH cells when motion stimuli of 15-s duration were presented (Dürr and Egelhaaf 1999).

The addition of exogenous Ca^{2+} buffer capacity to the cytosol alters Ca^{2+} dynamics and therefore hampers the interpretation of Ca^{2+} signals measured with fluorescent dyes. In contrast to whole cell patch-clamp recordings, the exact amount of Ca^{2+} indicator added to the cytosol cannot be controlled precisely when using sharp electrodes. Nevertheless, the influence of added Ca^{2+} buffers on Ca^{2+} dynamics can be assessed by comparing Ca^{2+} signals measured with indicators that differ in their affinity to Ca^{2+} . In fly TCs, the major effect of increased buffer capacity is a deceleration of $\Delta F/F$ decay

time courses. However, a dependence of Ca^{2+} dynamics on neuritic size can be observed both with high- and low-affinity indicators. This cannot be taken for granted, since endogenous Ca^{2+} buffers are typically less mobile than Ca^{2+} indicator dyes. Therefore the most likely effect of high concentrations of added buffers is increased diffusion of Ca^{2+} in the cytosol, which would reduce spatial inhomogeneities in Ca^{2+} dynamics (Holthoff et al. 2002; Sala and Hernandez-Cruz 1990). Furthermore, high-affinity Ca^{2+} dyes are much more prone to saturation than low-affinity dyes. Again, saturation would lead to an underestimation of the spatial differences in Ca^{2+} dynamics, because $[\text{Ca}^{2+}]$ reaches higher values in smaller neurites than in the major branches. Actual $\Delta[\text{Ca}^{2+}]$ in thin TC neurites might therefore reach higher levels and recover more rapidly than indicated by my experimentally determined $\Delta F/F$ time courses.

Functional relevance of $[\text{Ca}^{2+}]$ decay kinetics

The dynamics of Ca^{2+} clearance differs across spatial locations both in the dendrite and in the output area of fly TCs. The functional consequences of these findings may be different for the two cellular regions. Both HS and VS cells have been shown to possess chemical synapses in their output area (Hausen et al. 1980). At least for some VS cells, it has been shown by dual recordings with a postsynaptic target, the V1 neuron, that signal transmission operates fairly linearly within the natural activity range, i.e., when sensory stimuli are processed, both for constant motion stimulation and dynamically changing velocities (Kurtz et al. 2001; Warzecha et al. 2003). Interestingly, the Ca^{2+} channels in TCs have been found to be of the low-voltage-activated (LVA) type and are either slowly or noninactivating (Haag and Borst 2000). These properties may support sustained transmission of slow presynaptic voltage fluctuations near resting potential. However, at the VS-V1 synapse, fast spike-like depolarizations are also transmitted reliably (Warzecha et al. 2003). Thus rapid Ca^{2+} clearance is required to prevent temporal smear of fast signals. In my study, Ca^{2+} clearance appears faster in fine presynaptic endings than in adjacent larger-diameter branches. Still, the measured Ca^{2+} signals are obviously much slower than the regulation of transmitter release. This is likely to be due to the limited spatial resolution of the optical methods, which do not allow measurements of Ca^{2+} sufficiently close to the site of transmitter release, and to the buffering properties of the Ca^{2+} indicator. Nevertheless, my measurements suggest that a simple increase in surface area-to-volume ratio in small presynaptic endings can help to accelerate Ca^{2+} clearance. With improved spatial resolution, the tendency of faster Ca^{2+} clearance in small-diameter arborizations could probably be observed to continue with presynaptic neurites of smaller and smaller diameter. This trend highlights the importance of fast Ca^{2+} clearance at the sites of transmitter release for rapid termination of synaptic transmission after the cessation of stimulus motion.

Dendritic Ca^{2+} accumulation in fly TCs was shown to be correlated with a long-lasting AHP that follows stimulation with motion in the PD (Kurtz et al. 2000). This AHP may well form the physiological basis of a direction-selective component of motion adaptation (Harris et al. 2000; Kurtz et al. 2000), possibly caused by the opening of Ca^{2+} -dependent potassium channels (Sah and Faber 2002). Computationally, Ca^{2+} would

act as a temporal (and to a certain extent, spatial; see Dürr and Egelhaaf 1999) integrator, providing a cumulative build-up of adaptation during prolonged or repeated presentation of PD motion. The time course of Ca^{2+} clearance would determine the dynamics of direction-selective motion adaptation. Since the time constant of Ca^{2+} clearance decreases with decreasing diameter of dendritic branches, the time course of adaptation could vary across the dendrite, being transient in fine, distal arborizations and more sustained near the axon. A temporal aspect would thus be added to the capacity of TCs to keep adaptation spatially restricted to the stimulated parts of the receptive field (Maddess and Laughlin 1985).

ACKNOWLEDGMENTS

I thank M. Egelhaaf and J. Kalb for discussions throughout the course of this study and J. Waters and two anonymous reviewers for comments on earlier versions of this manuscript.

GRANTS

This work was supported by the Deutsche Forschungsgemeinschaft.

REFERENCES

- Berridge MJ.** Neuronal calcium signaling. *Neuron* 21: 13–26, 1998.
- Blaustein MP and Lederer WJ.** Sodium/calcium exchange: its physiological implications. *Physiol Rev* 79: 763–854, 1999.
- Borst A and Egelhaaf M.** In vivo imaging of calcium accumulation in fly interneurons as elicited by visual motion stimulation. *Proc Natl Acad Sci USA* 89: 4139–4143, 1992.
- Borst A and Haag J.** Neural networks in the cockpit of the fly. *J Comp Physiol [A]* 188: 419–437, 2002.
- Borst A and Single S.** Local current spread in electrically compact neurons of the fly. *Neurosci Lett* 285: 123–126, 2000.
- Carafoli E and Brini M.** Calcium pumps: structural basis for and mechanism of calcium transmembrane transport. *Curr Opin Chem Biol* 4: 152–161, 2000.
- Dürr V and Egelhaaf M.** In vivo calcium accumulation in presynaptic and postsynaptic dendrites of visual interneurons. *J Neurophysiol* 82: 3327–3338, 1999.
- Dürr V, Kurtz R, and Egelhaaf M.** Two classes of visual motion sensitive interneurons differ in direction and velocity dependency of in vivo calcium dynamics. *J Neurobiol* 46: 289–300, 2001.
- Egelhaaf M and Borst A.** A look into the cockpit of the fly: visual orientation, algorithms, and identified neurons. *J Neurosci* 13: 4563–4574, 1993a.
- Egelhaaf M and Borst A.** Movement detection in arthropods. *Rev Oculomot Res* 5: 53–77, 1993b.
- Egelhaaf M and Borst A.** Calcium accumulation in visual interneurons of the fly: stimulus dependence and relationship to membrane potential. *J Neurophysiol* 73: 2540–2552, 1995.
- Egelhaaf M, Borst A, Warzecha AK, Flecks S, and Wildemann A.** Neural circuit tuning fly visual neurons to motion of small objects. II. Input organization of inhibitory circuit elements revealed by electrophysiological and optical recording techniques. *J Neurophysiol* 69: 340–351, 1993.
- Egelhaaf M, Kern R, Krapp HG, Kretzberg J, Kurtz R, and Warzecha A-K.** Neural encoding of behaviourally relevant visual-motion information in the fly. *Trends Neurosci* 25: 96–102, 2002.
- Ellis-Davies GC and Kaplan JH.** Nitrophenyl-EGTA, a photolabile chelator that selectively binds Ca^{2+} with high affinity and releases it rapidly upon photolysis. *Proc Natl Acad Sci USA* 91: 187–191, 1994.
- Escobar AL, Velez P, Kim AM, Cifuentes F, Fill M, and Vergara JL.** Kinetic properties of DM-nitrophen and calcium indicators: rapid transient response to flash photolysis. *Pfluegers Arch* 434: 615–631, 1997.
- Fossier P, Tauc L, and Baux G.** Calcium transients and neurotransmitter release at an identified synapse. *Trends Neurosci* 22: 161–166, 1999.
- Gauk V, Egelhaaf M, and Borst A.** Synapse distribution on VCH, an inhibitory, motion-sensitive interneuron in the fly visual system. *J Comp Neurol* 381: 489–499, 1997.
- Haag J and Borst A.** Spatial distribution and characteristics of voltage-gated calcium signals within visual interneurons. *J Neurophysiol* 83: 1039–1051, 2000.

- Haag J and Borst A.** Recurrent network interactions underlying flow-field selectivity of visual interneurons. *J Neurosci* 21: 5685–5692, 2001.
- Haag J and Borst A.** Dendro-dendritic interactions between motion-sensitive large-field neurons in the fly. *J Neurosci* 22: 3227–3233, 2002.
- Harris RA, O'Carroll DC, and Laughlin SB.** Contrast gain reduction in fly motion adaptation. *Neuron* 28: 595–606, 2000.
- Haugland RP.** *Handbook of Fluorescent Probes and Research Products*. Eugene, OR: Molecular Probes, 2002.
- Hausen K.** Motion sensitive interneurons in the optomotor system of the fly. I. The horizontal cells: structure and signals. *Biol Cybern* 45: 143–156, 1982a.
- Hausen K.** Motion sensitive interneurons in the optomotor system of the fly. II. The horizontal cells: receptive field organization and response characteristics. *Biol Cybern* 46: 67–79, 1982b.
- Hausen K.** The lobula-complex of the fly: structure, function and significance in visual behaviour. In: *Photoreception and Vision in Invertebrates*, edited by Ali MA. New York: Plenum Press, 1984, p. 523–559.
- Hausen K and Egelhaaf M.** Neural mechanisms of visual course control in insects. In: *Facets of Vision*, edited by Stavenga DG and Hardie RC. Berlin: Springer, 1989, p. 391–424.
- Hausen K, Wobburg-Buchholz W, and Ribl WA.** The synaptic organization of visual interneurons in the lobula complex of flies. A light and electron microscopic study using silver- intensified cobalt-impregnations. *Cell Tissue Res* 208: 371–387, 1980.
- Hengstenberg R.** Common visual response properties of giant vertical cells in the lobula plate of the blowfly *Calliphora*. *J Comp Physiol [A]* 149: 179–193, 1982.
- Hengstenberg R, Hausen K, and Hengstenberg B.** The number and structure of giant vertical cells (VS) in the lobula plate of the blowfly *Calliphora erythrocephala*. *J Comp Physiol [A]* 149: 163–177, 1982.
- Herrington J, Park YB, Babcock DF, and Hille B.** Dominant role of mitochondria in clearance of large Ca²⁺ loads from rat adrenal chromaffin cells. *Neuron* 16: 219–228, 1996.
- Holthoff K, Tsay D, and Yuste R.** Calcium dynamics of spines depend on their dendritic location. *Neuron* 33: 425–437, 2002.
- Horstmann W, Egelhaaf M, and Warzecha AK.** Synaptic interactions increase optic flow specificity. *Eur J Neurosci* 12: 2157–2165, 2000.
- Kaplan JH and Ellis-Davies GC.** Photolabile chelators for the rapid photorelease of divalent cations. *Proc Natl Acad Sci USA* 85: 6571–6575, 1988.
- Krapp HG, Hengstenberg B, and Hengstenberg R.** Dendritic structure and receptive-field organization of optic flow processing interneurons in the fly. *J Neurophysiol* 79: 1902–1917, 1998.
- Kurtz R, Dürr V, and Egelhaaf M.** Dendritic calcium accumulation associated with direction-selective adaptation in visual motion-sensitive neurons in vivo. *J Neurophysiol* 84: 1914–1923, 2000.
- Kurtz R, Warzecha AK, and Egelhaaf M.** Transfer of visual motion information via graded synapses operates linearly in the natural activity range. *J Neurosci* 21: 6957–6966, 2001.
- Lev-Ram V, Miyakawa H, Lasser-Ross N, and Ross WN.** Calcium transients in cerebellar Purkinje neurons evoked by intracellular stimulation. *J Neurophysiol* 68: 1167–1177, 1992.
- Maddess T and Laughlin SB.** Adaptation of the motion-sensitive neuron H1 is generated locally and governed by contrast frequency. *Proc R Soc Lond B Biol Sci* 228: 251–275, 1985.
- Maeda H, Ellis-Davies GC, Ito K, Miyashita Y, and Kasai H.** Supralinear Ca²⁺ signaling by cooperative and mobile Ca²⁺ buffering in Purkinje neurons. *Neuron* 24: 989–1002, 1999.
- Majewska A, Brown E, Ross J, and Yuste R.** Mechanisms of calcium decay kinetics in hippocampal spines: role of spine calcium pumps and calcium diffusion through the spine neck in biochemical compartmentalization. *J Neurosci* 20: 1722–1734, 2000.
- Medler K and Gleason EL.** Mitochondrial Ca(2+) buffering regulates synaptic transmission between retinal amacrine cells. *J Neurophysiol* 87: 1426–1439, 2002.
- Nerbonne JM.** Caged compounds: tools for illuminating neuronal responses and connections. *Curr Opin Neurobiol* 6: 379–386, 1996.
- Oertner TG, Brotz TM, and Borst A.** Mechanisms of dendritic calcium signaling in fly neurons. *J Neurophysiol* 85: 439–447, 2001.
- Sabatini BL, Oertner TG, and Svoboda K.** The life cycle of Ca²⁺ ions in dendritic spines. *Neuron* 33: 439–452, 2002.
- Sah P and Faber ESL.** Channels underlying neuronal calcium-activated potassium currents. *Prog Neurobiol* 66: 345–353, 2002.
- Sala F and Hernandez-Cruz A.** Calcium diffusion modeling in a spherical neuron. Relevance of buffering properties. *Biophys J* 57: 313–324, 1990.
- Single S and Borst A.** Dendritic integration and its role in computing image velocity. *Science* 281: 1848–1850, 1998.
- Single S and Borst A.** Different mechanisms of calcium entry within different dendritic compartments. *J Neurophysiol* 87: 1616–1624, 2002.
- Sjostrom PJ and Nelson SB.** Spike timing, calcium signals and synaptic plasticity. *Curr Opin Neurobiol* 12: 305–314, 2002.
- Stanley EF.** The calcium channel and the organization of the presynaptic transmitter release face. *Trends Neurosci* 20: 404–409, 1997.
- Südhof TC.** The synaptic vesicle cycle: a cascade of protein-protein interactions. *Nature* 375: 645–653, 1995.
- Thomas D, Tovey SC, Collins TJ, Bootman MD, Berridge MJ, and Lipp P.** A comparison of fluorescent Ca²⁺ indicator properties and their use in measuring elementary and global Ca²⁺ signals. *Cell Calcium* 28: 213–223, 2000.
- von Gersdorff H and Matthews G.** Electrophysiology of synaptic vesicle cycling. *Annu Rev Physiol* 61: 725–752, 1999.
- Vranesic I and Knöpfel T.** Calculation of calcium dynamics from single wavelength fura-2 fluorescence recordings. *Pfluegers Arch* 418: 184–189, 1991.
- Warzecha AK, Egelhaaf M, and Borst A.** Neural circuit tuning fly visual interneurons to motion of small objects. I. Dissection of the circuit by pharmacological and photoinactivation techniques. *J Neurophysiol* 69: 329–339, 1993.
- Warzecha AK, Kurtz R, and Egelhaaf M.** Synaptic transfer of dynamic motion information between identified neurons in the visual system of the blowfly. *Neuroscience* 119: 1103–1112, 2003.
- Zucker RS.** Calcium- and activity-dependent synaptic plasticity. *Curr Opin Neurobiol* 9: 305–313, 1999.